

# THz emission from intrinsic Josephson junctions at zero magnetic field via breather auto-oscillations.

V. M. Krasnov

*Department of Physics, AlbaNova University Center,  
Stockholm University, SE-10691 Stockholm, Sweden*

I propose a new mechanism of intense high-frequency electromagnetic wave generation by spatially uniform stacked Josephson junctions at zero magnetic field. The ac-Josephson effect converts the dc-bias voltage into ac-supercurrent, however, in the absence of spatial variation of Josephson phase difference, does not provide dc-to-ac power conversion, needed for emission of electromagnetic waves. Here I demonstrate that at geometrical resonance conditions, the spatial homogeneity of phase can be spontaneously broken by appearance of breathers (bound fluxon-antifluxon pairs), facilitating effective dc-to-ac power conversion. The proposed mechanism explains all major features of recently observed THz radiation from large area  $\text{Bi}_2\text{Sr}_2\text{CaCu}_2\text{O}_{8+x}$  mesa structures.

Auto-oscillations are self-sustaining oscillations in nonlinear systems with frequency and often amplitude independent of driving force. Oscillatory behavior in plasma [1], operation of a clock and multivibrators, voice and sound of musical instruments, all are examples of auto-oscillations. Typically, periodic auto-oscillations are excited by a constant force. The frequency is determined either by an internal resonance (e.g. a cavity mode), or a characteristic relaxation time. Auto-oscillations are widely used for generation of microwaves, e.g. in Gunn diodes, magnetrons and klystrons.

Recently a significant THz emission has been reported at zero magnetic field from large area  $\text{Bi}_2\text{Sr}_2\text{CaCu}_2\text{O}_{8+x}$  (Bi-2212) mesa structures [2, 3], which represent natural stacks of atomic-scale intrinsic Josephson junctions (IJJs). Although the emission occurs at geometrical (Fiske) resonance frequencies, association with conventional Fiske steps [4] is problematic because their amplitude is zero at  $H = 0$ . Furthermore, significant emission power would require a large quality factor  $Q \gg 1$  [5]. Since  $Q$  of Fiske steps is inversely proportional to the mesa size [4], it is not clear how it could be sufficiently large for large mesas at large operation temperatures and quasiparticle damping due to large self-heating. Therefore, the observed radiation is quite puzzling and remains a matter of intense discussion [5–12].

In this letter I propose a new mechanism of emission from a spatially uniform stack of Josephson junctions at zero applied field. It is shown that at geometrical resonance conditions the homogeneous state becomes unstable with respect to formation of a breather lattice in the stack. Breathers are bound fluxon-antifluxon pairs [13]. They effectively couple the dc-bias to the ac-Josephson oscillations and makes resonances self-sustainable, once ignited. It is argued that the discovered breather auto-oscillations explain experimental features of the zero-field emission from large Bi-2212 mesas.

Radiation from large IJJs is following the ac-Josephson relation [2, 3]. Although the ac-Josephson effect converts the dc-bias voltage into the oscillating supercur-

rent, this does not ensure radiation from junctions because the supercurrent is non-dissipative and can not by itself pump energy from the dc-power supply into radiation. Such a dc-to-ac power conversion can be achieved via the Lorentz force

$$F_L = sI \times B, \quad (1)$$

(per junction), where  $I$  is the dc-bias current and  $s$  is the stacking periodicity ( $s \simeq 1.5$  nm for IJJs). Therefore, emission by means of the ac-Josephson effect requires finite  $B_i(x) \neq 0$ , which is connected with the finite Josephson phase gradients  $\nabla\varphi_i \neq 0$  ( $i$  is the junction index).

Structural inhomogeneity may lead to some coupling of the dc-bias to the ac-resonance field at  $H = 0$  [7, 14]. The inhomogeneity can be caused by variation of the critical current density, or nonuniform bias current distribution [15]. In large Bi-2212 mesas the inhomogeneity can also be induced by uneven self-heating at large bias [9] and by defects in Bi-2212 single crystals. Associated phase gradients can be attributed to self-field caused by nonuniform current flow. This may lead to appearance zero-field Fiske steps [14]. However, the observed emission is hardly explained by zero-field Fiske steps: large flux quantization field in atomic scale IJJs would require very large inhomogeneity [7]. Furthermore, such inhomogeneity could hinder mutual synchronization of IJJs [4] and suppress collective Fiske resonances, required for coherent amplification of the emission power.

Fluxons create a large phase gradient  $\simeq \pi/\lambda_J$  ( $\lambda_J$  is the Josephson penetration depth) and thus provide an effective dc-to-ac-power conversion. Usually fluxons are introduced by applying in-plane magnetic field. In long Josephson junctions,  $L \gg \lambda_J$ , they can be trapped at  $H = 0$ . Emission scenarios, involving quasistatic semi-fluxons/antifluxons [6], or fluxons/antifluxons [8] in mesas, were proposed. For a single junction static fluxon-antifluxon pairs are unstable, because they tend to collapse and annihilate. But for stacked junction fluxon-antifluxon pairs in neighbour junctions are stable [16, 17]. Fluxon-antifluxon modes at  $H = 0$  has been clearly ob-

served in large Bi-2212 mesas, as they cause multiple valued critical current [16]. Fluxons experience the Lorentz force, which facilitates efficient pumping of dc-power into kinetic energy of fluxons. Upon collision and annihilation of fluxons at junction edges, radiation pulses are produced. The corresponding flux-flow emission is well studied for single junctions [18]. Significant flux-flow emission from stacked junctions requires both stabilization of the square fluxon lattice and high quality geometrical resonances [5], because the emission power is  $P_{rad} \propto Q^2$  and the linewidth  $\propto Q^{-1}$ . For IJJs, this can only be achieved at strong fields  $H > \Phi_0/\lambda_{Js} \simeq 2T$ , and for small Bi-2212 mesas [4, 19]. None of those requirements is realized in case of zero-field emission from large mesas.

Several non-Josephson emission mechanisms at  $H = 0$  are also known. Stable fluxon-antifluxon pairs in stacked junctions can be unbound by a large enough transport current and may start shuttling in the stack, leading to appearance of zero-field steps (ZFS) in  $I - V$  curves [17]. Some emission of electromagnetic waves does occur at ZFS [20, 21], however, it occurs at subharmonics of the Josephson frequency [20] and the emission power is small because the fluxon is not annihilated upon collision with the edge, but is reflected as an antifluxon. Therefore, unlike in the flux-flow case, only a minor part of fluxons energy can be radiated. Moreover, emission power at ZFS can not be large because the fluxon will not be reflected if it will lose significant part of its energy upon the collision with the edge [13]. In stacks, ZFS can be accompanied by non-Josephson Cherenkov radiation [22, 23] due to partial decomposition of fluxons into travelling plasma waves [23, 24]. Also, recombination of injected nonequilibrium quasiparticles leads to generation of bosons [25, 26]. The nonequilibrium emission is direct (does not involve the ac-Josephson effect) and can provide very high efficacy [27]. It is most effective at  $H = 0$  because it benefits from the sharp gap singularity in the quasiparticle density of states.

Analysis of emission from stacked Josephson junctions requires implementation of proper radiative boundary conditions into the coupled sine-Gordon equation. In the numerical simulations, presented below, non-local radiative boundary conditions, derived in Ref. [5], are employed. The emission is facilitated by the finite radiation impedance  $Z$ . Simulations are made for a stack of  $N = 10$  identical, uniform junctions with parameters typical for optimally doped Bi-2212 IJJs [4, 19]. The damping parameter was varied from strongly underdamped  $\alpha = 0.01$  to overdamped  $\alpha = 1$ . Note that IJJs exhibit hysteresis in  $I-V$  characteristics, i.e., remain underdamped, almost up to  $T_c$  [28]. The emission power is scaling with the width of the stack  $w$  and is normalized to  $w = 20\mu\text{m}$ .

Figure 1 (a) shows  $I-V$  characteristics for stacks with the length  $L = 20\lambda_J$  for  $\alpha = 0.01$  (black, gray and blue) and 0.1 (red, magenta). Different colors represent simulations with different initial conditions, corresponding to

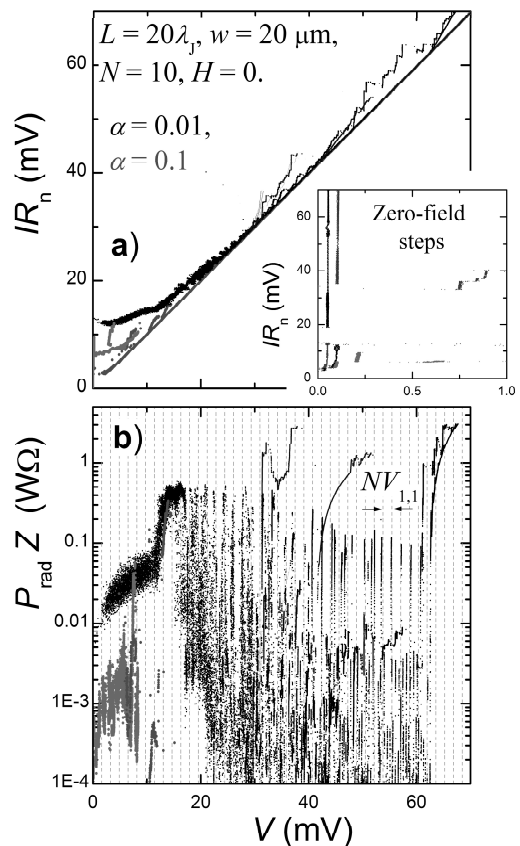


FIG. 1. (Color online). (a) Normalized  $I-V$  characteristics for long, uniform, underdamped stack Josephson junctions at zero applied field. Appearance of pronounced steps, caused by breather auto-oscillations, is seen. Different colors correspond to simulations with different initial conditions with certain amount of trapped fluxons/antifluxons. Inset shows zero-field steps at low voltages. (b) Normalized radiative power along the same  $I-V$ 's. Pronounced maxima occur at collective in-phase cavity resonances, indicated by grid lines.

certain amount of trapped fluxons and antifluxons. At low bias this leads to appearance of ZFS [17], shown in the inset. At larger bias, distinct resonances appear, resembling Fiske steps.

Figure 1 (b) shows the radiation power  $P_{rad}$  (from one edge), normalized by the radiation impedance  $Z$ . All presented simulations are made for very large  $Z$ , so that radiative losses are much smaller than internal resistive losses. Under those circumstances, the product  $P_{rad}Z$  is constant [5]. From comparison of Figs. 1 (a) and (b) it is seen that some steps are accompanied by strong emission, others to the contrary, correspond to emission minima. Distinct emission maxima occur at voltages of collective in-phase Fiske steps, shown by the grid in Fig. 1 (b).

Figure 2 shows snapshots of spatial distributions of phases  $\varphi_i$  (top panels), magnetic inductions  $B_i$  (middle panels,  $\simeq 0.184\text{Gs}$  per division) and ac-components of

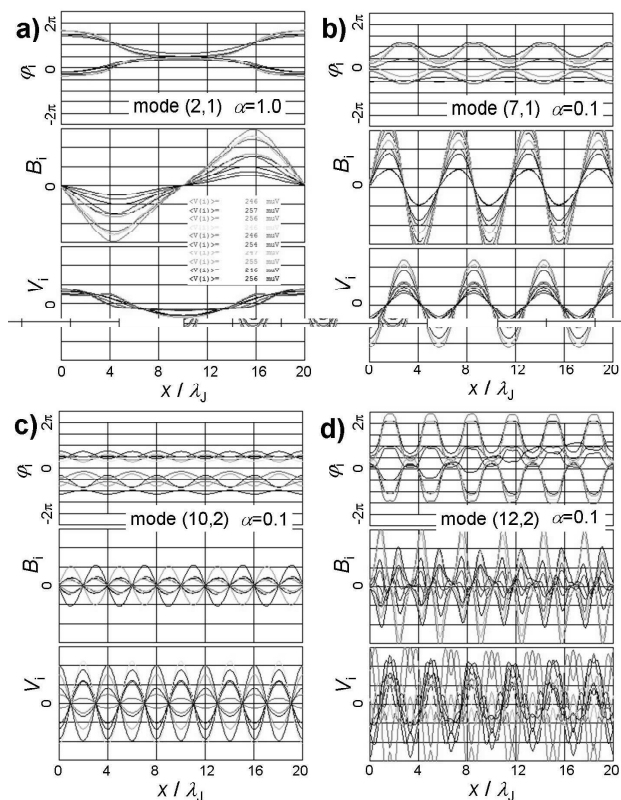


FIG. 2. (Color online). Snapshots of phase (top panels), magnetic induction (middle panels) and ac-component of voltage (bottom panels) at for different resonances for  $L = 20\lambda_J$  overdamped  $\alpha = 1$  (a) and underdamped  $\alpha = 0.1$  (b-d) stacks. It is seen that electromagnetic field forms standing-wave patterns in the stack. Resonant cavity modes  $(m, n)$  are indicated in the figures.

voltages  $V_i$  in each junction (bottom panels,  $\simeq 209\mu\text{V}$  per division) at for different resonances for (a) overdamped  $\alpha = 1$  and (b-d) underdamped  $\alpha = 0.1$  stacks with  $L = 20\lambda_J$ . The junction color code is represented by the dc-voltage annotation in Fig. 2 (a). It is seen that electromagnetic field forms two-dimensional standing wave patterns in the stack, similar to Fiske resonances [4, 5, 29]. Resonant modes  $(m, n)$  are characterized by the wave numbers  $k_{ab} = m\pi/L$  in-plane and  $k_c = n\pi/Ns$  in the  $c$ -axis direction [29].

From Fig. 2 it is seen that there is no increment of phase in the junctions  $\varphi_i(x=0) = \varphi_i(L)$ , which means that the net magnetic flux in each junction is zero. The observed modulation of phase is, therefore, caused by a spontaneous formation of ordered breather lattice, consisting of similar breather chains in each junction. Breather chains couple to the dc-power supply via the Lorentz force and effectively pump energy into ac-Josephson oscillations. This makes breather resonances self-sustaining, once ignited. The frequency of oscilla-

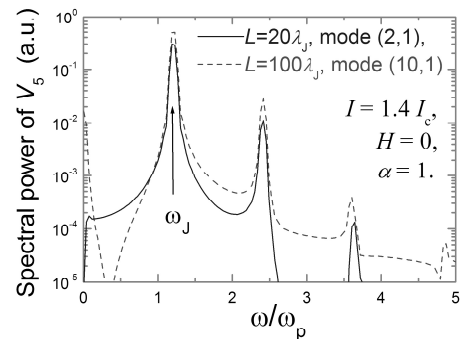


FIG. 3. (Color online). Spectra of voltage oscillations in the middle junction for overdamped stacks,  $\alpha = 1$ , with  $L = 20\lambda_J$  and  $100\lambda_J$ . Stacks are biased at the same dc-voltage, corresponding to in-phase cavity modes  $(2,1)$  and  $(10,1)$ , respectively. Spectra are similar and have narrow maxima at the Josephson frequency  $\omega_J$ . Note that amplitudes and linewidths of the two resonances are similar, despite different  $L$ .

tions is adopted to the nearest cavity mode in the stack. Such behavior is typical for auto-oscillation phenomena, as mentioned in the introduction. Therefore, I refer the discovered new type of zero-field resonances to as breather auto-oscillations.

The breather amplitude is not quantized and the phase variation can acquire any value in the range  $-2\pi < \Delta\varphi_i < 2\pi$ . Fig. 2 (a) represents a special case, when the phase amplitude at a certain time is close to  $\pm\pi$ , similar to the case discussed in Ref. [6]. Fig. 2 (d) shows another special case when fluxons and antfluxons in the breather are well separated and the amplitude  $\Delta\varphi_i \simeq \pm 2\pi$ , similar to the case considered in Ref. [8]. However, even in those cases, it should be realized that  $\Delta\varphi_i$  are not constant but are oscillating in time. In general the amplitude  $\Delta\varphi_i$  can be arbitrary, as shown in Figs. 2 (b,c).

Figure 3 shows the spectra of voltage oscillations in the middle junction  $i = 5$  at the edge of the stack  $x = 0$ . Frequency is normalized by the Josephson plasma frequency  $\omega_p$ . Results are shown for two overdamped stacks  $\alpha = 1$  with different lengths  $L = 20\lambda_J$  (solid line) and  $L = 100\lambda_J$  (dashed line), biased at the same relative current  $I/I_c = 1.4$  and having the same voltage. For  $L = 20\lambda_J$  it corresponds to the in-phase resonance  $(2,1)$ , shown in Fig. 2 (a), and for  $L = 100\lambda_J$  to the in-phase mode  $(10,1)$ , with the same spatial separation between nodes. It is seen that in both cases the radiation spectra are similar and consist of a sharp maximum at the primary Josephson frequency, marked by the upward arrow, and several small harmonics.

Simulations in Fig. 3 demonstrate that breather auto-oscillations are not hampered even in the overdamped case  $\alpha = 1$  and in very long stacks. Furthermore, neither the amplitude, nor the linewidth of oscillations is deteriorated in the longer stack. This implies that quality

factors of the two resonances are similar. Quality factors of geometrical resonances were considered in Ref. [4]: for the mode  $(m, n)$ ,  $Q_{m,n} = m\pi(c_n/c_0)(\lambda/L)/\alpha$ , where  $c_n$  is the velocity of mode  $n$  and  $c_0$  is the Swihart velocity of a single junction. The in-phase mode  $n = 1$  is the most important for achieving coherent high power emission. Using the approximate expression for  $c_1$  [4], we obtain

$$Q_{m,1} \simeq \frac{m\sqrt{2}(N+1)}{(L/\lambda_j)\alpha}, \quad (2)$$

valid for  $N < \pi\lambda_{ab}/s \simeq 400$ , where  $\lambda_{ab} \simeq 200\text{nm}$  is the London penetration depth. It is seen that modes with the same  $L/m$  from Fig. 3 indeed have the same  $Q \simeq \sqrt{2} > 1$ , despite junctions are long and overdamped. The quality factor of the junction,  $Q_0 \equiv Q(\omega = \omega_p) = 1/\alpha$ , should not be confused with the quality factor of geometrical resonances  $Q_{m,n} = (\omega_{m,n}/\omega_p)Q_0$ .

In conclusion, a new mechanism of zero-field radiation from stacked Josephson junctions is proposed, via spontaneous breather auto-oscillations at geometrical resonance conditions [30]. It explains all major experimental features of THz emission from large Bi-2212 mesas [2, 3]:

i) Breather auto-oscillations lead to powerful coherent radiation from uniform mesas at zero magnetic field, because breather can effectively couple ac-Josephson oscillations to dc-power supply via the Lorentz force.

ii) They excite conventional cavity modes in the stack with the frequency following the ac-Josephson relation and inversely proportional to the junction length.

iii) Coherent flux-flow emission requires stabilization of the rectangular (in-phase) fluxon lattice, which is counteracted by fluxon-fluxon repulsion [19]. Establishment of in-phase breather oscillations is much easier because of much smaller breather-breather repulsion.

iv) Unlike conventional Fiske resonances, which have only one strong mode for a given field (the velocity matching mode with two nodes per fluxon) [4], the wavelength of breather chain can be arbitrary. This flexibility provides an important advantage with respect to Fiske resonances, because it allows maximum amplitude for any geometrical resonance at  $H = 0$ .

v) The flexibility of breather resonances ensures that some, high enough, in-phase resonances would have large quality factor, irrespective of the damping parameter or the junctions length. This allows intense coherent emission of electromagnetic waves with narrow linewidth even in very large mesas and at elevated temperatures.

vi) Emission due to breather auto-oscillations is suppressed by small in-plane magnetic field. Numerical simulations (not shown) demonstrated that with increasing field, breather resonances are gradually substituted by conventional Fiske resonances, which have smaller amplitude at low fields.

vii) Breather resonances depend on initial conditions, which resembles metastability of emission from Bi-2212

mesas. Essentially breather auto-oscillations need to be ignited to become self-sustainable. Here they were ignited with the help of trapped fluxons/antifluxons. In experimental situation it is likely that the ignition is facilitated by the non-equilibrium mechanism [25–27], which is most intense at large injection current densities just beneath electrodes, as seen in laser microscopy [3].

viii) From Eq. (2) it follows that coherent emission is improved in mesas with larger number of IJJs, up to  $N \simeq 400$ , which is the optimal number for achieving large emission power, without too large self-heating.

- 
- [1] S.K.Zhdanov et.al., New J. Phys. 12, 043006 (2010).
  - [2] L. Ozyuzer et al., Science 318, 1291 (2007).
  - [3] H. B. Wang *et al.*, Phys. Rev. Lett. 105, 057002 (2010).
  - [4] S.O. Katterwe et al., Phys. Rev. B 82, 024517 (2010).
  - [5] V. M. Krasnov, Phys. Rev. B 82, 0134524 (2010).
  - [6] X. Hu and S.Z. Lin, Supercond. Sci. Techn. 23, 053001 (2010).
  - [7] A. E. Koshelev and L. N. Bulaevskii, Phys. Rev. B 77, 014530 (2008).
  - [8] A.E. Koshelev, Phys. Rev. B 78, 174509 (2008).
  - [9] H. B. Wang *et al.*, Phys. Rev. Lett. 102, 017006 (2009).
  - [10] M. Tachiki, S. Fukuya and T. Koyama, Phys. Rev. Lett. 102, 127002 (2009).
  - [11] T. Tachiki, and T. Uchida, J. Appl. Phys. 107, 103920 (2010).
  - [12] R. A. Klemm and K. Kadowaki, J. Phys. Cond. Mat. 22, 375701 (2010).
  - [13] D. W. McLaughlin and A. C. Scott, Phys. Rev. A 18, 1652 (1978).
  - [14] C. Camerlingo, M. Russo and R. Vaglio, J. Appl. Phys. 53, 7609 (1982).
  - [15] V. M. Krasnov, V.A.Oboznov and N.F.Pedersen, Phys. Rev. B 55, 14486 (1997).
  - [16] V. M. Krasnov, et al., Phys. Rev. B 61, 766 (2000).
  - [17] R. Kleiner, T. Gaber and G.Hechtfisher, Phys. Rev. B 62, 4086 (2000).
  - [18] V.P. Koshelets and S.V. Shitov, Supercond. Sci.Technol. 13, R53 (2000).
  - [19] S.O. Katterwe and V.M. Krasnov, Phys. Rev. B 80, 020502(R) (2009).
  - [20] B.Dueholm, et al., Phys. Rev. Lett. 46, 1299 (1981).
  - [21] J. J. Chang, J.T. Chen, M.R. Scheuermann and D.J. Scalapino, Phys. Rev. B 31, 1658 (1985).
  - [22] G. Hechtfisher, R. Kleiner, A.V. Ustinov, and P. Müller, Phys. Rev. Lett. 79, 1365 (1997).
  - [23] V.M. Krasnov and D. Winkler, Phys. Rev. B 56, 9106 (1997).
  - [24] V.M. Krasnov, Phys. Rev. B 63, 064519 (2001).
  - [25] I. Iguchi, et al., Phys. Rev. B 61, 689 (2000).
  - [26] V. M. Krasnov, Phys. Rev. Lett. 97, 257003 (2006).
  - [27] V. M. Krasnov, Phys. Rev. Lett. 103, 227002 (2009).
  - [28] V. M. Krasnov, T.Golod, T.Bauch and P.Delsing, Phys. Rev. B 76, 224517 (2007).
  - [29] R. Kleiner, Phys. Rev. B 50, 6919 (1994).
  - [30] The variety of dynamic states in stacked junctions can be seen form the provided demo-program: <http://ekmf.physto.se/TMP/DemoRadiative.zip>